Amended paper of session U052, Ultrawideband Communication I, *Proceedings of MILCOM*, 2004.

A SYNCHRONIZING SCHEME FOR AN IMPULSE NETWORK

Chee-Cheon Chui and Robert A. Scholtz
UltRaLab, Communication Sciences Institute, USC
Los Angeles, CA 90089-2565
{ccheeche@dso.org.sg; scholtz@usc.edu}

ABSTRACT

We define a Synchronous Impulse Network (SIN) to be a network of distributed wireless nodes employing UWB impulse transceivers whose local oscillators are 'ticking' at the same time/phase. In this paper, a synchronizing scheme employing Time-of-Arrival (ToA) measurements to transfer time among nodes in order to build a SIN is proposed. Three major sources of impairments to the measurement of the ToA are considered. They are additive noise, multipath self-interference and Non-Line-Of-Sight (NLOS) measurements. The effect of multipath self-interference on a correlative timing detector, which is an important component of the proposed synchronization system, has been addressed in [8]. This paper is devoted to the proposed master-slave Time Division Multiple Access (TDMA) synchronization scheme and analyzes the accumulated timing jitter as a result of additive noise, oscillator phase noise and multipath propagation, and places a bound on the number of synchronous nodes possible in the network. We will conclude this paper by introducing the concept of a 'roving' master which transforms the master-slave TDMA scheme to a mutual synchronous network. The other objectives of the 'roving' master are to extend the geographical coverage of the synchronous network and overcome blockages of signal propagation paths.

INTRODUCTION

A Synchronous Impulse Network (SIN) is defined to be a network of distributed wireless nodes employing UWB impulse transceivers whose local oscillators are 'ticking' at the same time/phase. To attain timing synchronization, we propose a synchronizing scheme employing Time-of-Arrival (ToA) measurements to effect time transfer among nodes in the network. There exist time transfer techniques such as one-way, common-view and two-way time transfer [4]. The proposed scheme is a combination of one-way synchronization from the master node to the slave nodes followed by two-way ranging using the master as the transponder.

We note that network time transfer is a much researched topic since the 1960s [3]. Recently, [5] highlights the importance and applications of network synchronization in large-scale telecommunication systems. The works cited in [3] provide a mathematical model of the synchronization problem in a distributed network and address its stability. Reference [14] utilizes UWB impulses to synchronize nodes uniformly distribution in a squared region ignoring propagation delay as the area covered by the network is assumed to be small. We take a system specific approach here, i.e., we start by restricting ourselves to using UWB impulses and the ultra-wide bandwidth of such signals naturally suggests a TDMA scheme for communications in the network. We then proceed to analyze the timing performance of the network attained using the proposed synchronizing scheme. Notably, our work differs from [3] in the sense that there is only one physical channel for time transfer among nodes in the network and logical channels are formed via time division multiplexing. Therefore the temporal domain, crucial to the performance of the proposed SIN, is the new dimension addressed herein that has not being addressed previously in the open literature.

We considered three major sources of impairments to the measurement of the ToA. They are additive noise (e.g., receiver noise), oscillator phase noise, multipath self-interference and NLOS measurements that give a positive bias to the ToA readings [9]. A correlative timing detector [7] that correlates the received signal with a reference signal generated at the receiver is used to measure the ToA. No feedback error-tracking loop is assumed in the analysis else the timing jitter would have to be modified by the loop noise bandwidth [3]. For UWB impulses fully utilizing the FCC indoor spectral mask, the bias on the ToA measurements attributed to multipath self interference is assumed negligible [8].

The results will be of interest considering the fact that time transfer using UWB impulses has these advantages: (a) finer time resolution, (b) ability to resolve multipath and (c) the low probability of intercept and detection (LPI/LPD) of such signals. It is pointed out in [4] that a propagation channel that can be characterized easily is pivotal to good practical performance for time transfer system. In most channels envisioned, UWB transceivers sending sufficiently narrow impulses do not suffer adversely from inter-pulse interference, and therefore are likely to perform better than conventional carrier based continuous narrowband signals which are often degraded by inter-symbol interference.

This work is supported in part by a MURI Project under Contract DAAD 19-01-1-0477 from the US Army Research Office. Chee-Cheon Chui's postgraduate study in USC is supported by DSO National Laboratories, Singapore.

SYSTEM MODEL

The imperfect timing function generated by transceiver (s)'s local oscillator is modeled as in [2] and [15]:

$$T^{(s)}(t)=\sum_{v=1}^{V}\breve{a}_v^{(s)}t^v/v!-\breve{d}^{(s)}+(\breve{\varphi}^{(s)}(t)-\breve{\varphi}^{(s)}(0))/\omega_o \quad (1)$$

where t represents the true time, ω_o is the oscillator nominal frequency, $\breve{a}_v$ are the coefficients characterizing the oscillator, $\breve{d}^{(s)}$ the initial timing offset of the oscillator and $\breve{\varphi}(t)$ the random phase jitter also known as the short-term instabilities with zero mean. An oscillator is said to be perfect if its timing function is given by $T^{(s)}(t)=t-\breve{d}^{(s)}$. The positive-going zero crossings of an oscillator with timing function given by (1) are used to trigger the transmission of UWB impulses. Therefore the receive and reference UWB signals at receiver (s) are modeled as:

$$y^{(s)}(t)=A_w^{(s)}\sum_{k'}w\left(T^{(m)}(t-\tau_{m,s}-\rho_{m,s})-k'T_f\right)+n(t) \quad (2a)$$

$$f^{(s)}(t)=A_r^{(s)}\sum_{k}r\left(T^{(s)}(t)-kT_f\right) \quad (2b)$$

where $n(t)$ is the additive noise in the channel with one-sided density N_o, T_f is the frame period with one monocycle $w(\circ)$ per frame, A is the amplitude of the respective signals, $w(t)$, $r(t)$ are the received and reference monocycle waveforms with unit energy. In (2a), $\tau_{m,s}$ is used to explicitly denote the Line-Of-Sight (LOS) propagation delay from transceiver (m) to transceiver (s), and $\rho_{m,s}$ is the additional path length from Non-Line-Of-Sight (NLOS) propagation and is assumed to be a 'spatial' random variable with a positive mean. The term 'spatial' refers to the fact that randomness of $\rho_{m,s}$ arises from the random distribution of the nodes and their scattering environment. The purpose of defining the reference monocycle at the receiver will be made clear in (10). Subject to satisfying the bounds derived in (26)-(28), it is assumed that $k=k'$ in subsequent analysis.

TIME TRANSFER SCHEME

In Fig. 1, the time transfer scheme for two nodes in the network is illustrated assuming $\tau_{m,s}=\tau_{s,m}$. We denote the inverse function that maps the timing generated by the transceiver to true time by $\bar{T}^{(m)}(t')$ and $\bar{T}^{(s)}(t')$ for master node (m) and slave node (s) respectively.

The synchronizing scheme works as follows. The master starts by transmitting synchronizing pulses at $T^{(m)}(t_k^{(m)})=kT_f$ for $k\in\{0,...,K_s-1\}$ to all other transceivers in the network. The slave transceiver measures the ToA, denotes as $\Omega_{m,s(k)}^a$, of the k^{th} synchronizing pulse with respect to the start of its k^{th} frame at $T^{(s)}(t_k^{(s)})=kT_f$. Then:

$$\Omega_{m,s(k)}^a=\tau_{m,s}+\rho_{m,s}+\bar{T}^{(m)}(kT_f)-\bar{T}^{(s)}(kT_f)+\varepsilon_{(k)}^a \quad (3)$$

where $\varepsilon_{(k)}^a$ is the measurement noise associated with channel noise when determining the ToA of the k^{th} synchronizing pulse transmitted from the master triggered at $T^{(m)}(t_k^{(m)})=kT_f$. The subscript in bracket $(\circ)_{(k)}$ is used to indicate dependency on time of measurement. For example, $(\circ)_{(z,j)}$ indicates the z^{th} frame in the j^{th} slot assuming there are multiple frames ($K>1$), per slot.

If there are N transceivers in the network, then, in its assigned time slot, e.g., time slot j, $j\in\{2,...,N\}$ each slave transceiver will transmit K_r up-link ranging pulses in contiguous frames to the master. The ToA of the z^{th} pulse, $z\in\{0,...,K_r-1\}$, at the master with respect to the start of the z^{th} frame of the master 's j^{th} slot is:

$$\Omega_{s,m(z,j)}^b=\tau_{s,m}+\rho_{s,m}+\bar{T}^{(s)}(\theta_{up(z,j)}T_f)-\bar{T}^{(m)}(\theta_{up(z,j)}T_f)+\varepsilon_{(z,j)}^b \quad (4)$$

with frame index $\theta_{up(k,j)}=K_s+(j-2)K_r+z$ and $\varepsilon_{(z,j)}^b$ is the associated measurement noise.

The master will 'transpond' the received ranging pulse from individual slaves to the designated down-link time slot and re-transmit it as the return ranging pulse. If the

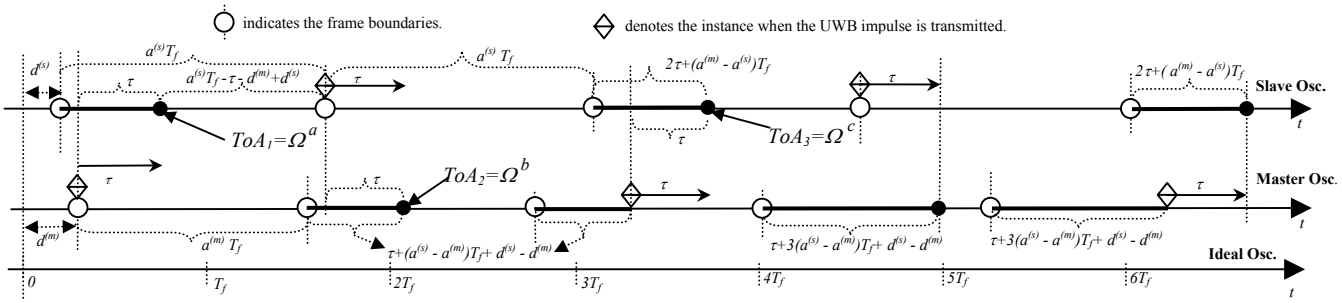

Figure 1: A jitter-free diagram illustrating the parameters used to compute the timing offset. For ease of illustration, $\breve{a}_v^{(s)}=0$ for $v>1$, $\forall s$. Timings generated by transceivers local oscillators are scaled by their respective drift rate $a_1^{(s)}$ while all annotated parameters such as τ, $d^{(m)}$ and $d^{(s)}$ are timed by the ideal oscillator. It is assumed that the width of the impulses, which is stretched by transmitter drift rate, does not affect determination of its ToA at the receiver. The parameters $a_1^{(s)}=1/\breve{a}_1^{(s)}$, $a_1^{(m)}=1/\breve{a}_1^{(m)}$, $d^{(m)}/\breve{a}_1^{(m)}$ and $d^{(s)}/\breve{a}_1^{(s)}$ are defined in (7).

down-link time slot is i, $i\in\{2,..,N\}$, i not necessarily equaling j, the ToA of the z^{th} return pulse at the slave is determine as $\Omega^{c}_{m,s(z,j,i)}$:

$$\begin{aligned}\Omega^{c}_{m,s(z,j,i)} &= \tau_{m,s}+\rho_{m,s}+\Omega^{b}_{s,m(z,j)}+\varepsilon^{c}_{(z,j,i)} \\ &\quad +\bar{T}^{(m)}(\theta_{dn(z,i)}T_f)-\bar{T}^{(s)}(\theta_{dn(z,i)}T_f)\end{aligned} \tag{5}$$

where $\theta_{dn(z,i)}=K_s+(N-1)K_r+(i-2)K_r+z$ is the frame index for the down-link transmission and $\varepsilon^{c}_{(z)}$ is the measurement noise. It is assumed that there is no inter-frame interference. The timing equation derived at the slave transceiver after transmitting the k^{th} synchronization pulse at the first time slot, and the z^{th} ranging pulse/frame at the j^{th} up-link and i^{th} down-link time slot is given by:

$$\vartheta_{m,s(k,z,j,i)}=\Omega^{c}_{m,s(z,j,i)}/2-\Omega^{a}_{m,s(k)} \tag{6}$$

The two-way ranging is to negate out the propagation delay τ between master and slaves transceivers.

In subsequent analysis, we restrict ourselves to analyzing the case in which $\breve{a}^{(s)}_{v}=0$, $v>1$, $\forall s$. Then

$$T^{(s)}(t)=\breve{a}^{(s)}_{1}t-\breve{d}^{(s)}+(\breve{\varphi}^{(s)}(t)-\breve{\varphi}^{(s)}(0))/\omega_o \tag{7a}$$

$$\bar{T}^{(s)}(t')=(t'+\breve{d}^{(s)}-(\breve{\varphi}^{(s)}(t)-\breve{\varphi}^{(s)}(0))/\omega_o)/\breve{a}^{(s)}_{1} \tag{7b}$$

where $T^{(s)}(t)=t'$. Letting $\varphi^{(s)}(t)=\breve{\varphi}^{(s)}(t)/\breve{a}^{(s)}_{1}$, $a^{(s)}_{1}=1/\breve{a}^{(s)}_{1}$, $d^{(s)}=\breve{d}^{(s)}/\breve{a}^{(s)}_{1}$, $d^{\delta}=d^{(m)}-d^{(s)}$ and $a^{\delta}_{1}=a^{(m)}_{1}-a^{(s)}_{1}$, (3), (4) and (5) reduce to the following:

$$\Omega^{a}_{m,s(k)}=\tau_{m,s}+\rho_{m,s}+d^{\delta}+a^{\delta}_{1}kT_f+\varepsilon^{a}_{(k)}-\mu_{(k)} \tag{8a}$$

$$\Omega^{b}_{s,m(z,j)}=\tau_{s,m}+\rho_{s,m}-d^{\delta}-a^{\delta}_{1}\theta_{up(z,j)}T_f+\varepsilon^{b}_{(z,j)}+\mu_{(\theta_{up(z,j)})} \tag{8b}$$

$$\begin{aligned}\Omega^{c}_{m,s(z,j,i)} &= \tau_{m,s}+\tau_{s,m}+\rho_{m,s}+\rho_{s,m}+\varepsilon^{c}_{(z,i)}+\varepsilon^{b}_{(z,j)}-\mu_{(\theta_{dn(z,i)})}+\mu_{(\theta_{up(z,j)})} \\ &\quad +a^{\delta}_{1}(\theta_{dn(z,i)}-\theta_{up(z,j)})T_f\end{aligned} \tag{8c}$$

where $\theta_{dn(z,i)}-\theta_{up(z,j)}=(N-1+i-j)K_r$, which is independent of the frame indices and $\mu_{(k)}$ is defined by:

$$\mu_{(k)}=\left(\varphi^{(m)}(t^{(m)}_{k})-\varphi^{(m)}(0)-\varphi^{(s)}(t^{(s)}_{k})+\varphi^{(s)}(0)\right)/\omega_o \tag{9}$$

MITIGATING OSCILLATOR DRIFT

We assume transceivers are stationary during time transfer. Then estimation of difference in oscillator drift can be accomplished by at least two different approaches.

One possible approach is to employ a second order Time Locked-Loop (TLL)/Delay Locked-Loop (DLL) as described in [7] and [2] at the slave transceivers to acquire and track the synchronizing pulses from the master. The master will send out a sufficiently long sequence (length K_s) of monocycles during the first time slot to be pulled-in and tracked by the TLL at the slave nodes, which will then estimate $(\tau+d^{\delta}+\rho)$ and $a^{\delta}_{1}T_f$.

The second approach can be viewed as a modification of the techniques described in [6]. The slave transceiver takes successively ToA measurements of the UWB pulses from the master. Then, instead of employing a second order TLL, a Least Squares (LS) fitting is performed on the recorded measurements to generate estimates for $a^{\delta}_{1}T_f$ and $(\tau+d^{\delta}+\rho)$.

The two approaches just described are not able to extract d^{δ} from $(\tau+d^{(m)}-d^{(s)}+\rho)$, hence the need for the up-link and down-link ranging pulses to negate out τ in (6).

The length of this paper does not allow us to discuss the two approaches fully. Instead, the LS estimator and its estimation variance are presented. Interested readers are referred to [2] and [6] for other details.

To perform LS estimation, it is assumed that a correlative timing detector described in [7] and shown in Fig. 2 is used to measure the ToA. The timing detector characteristic function is defined as:

$$g^{(s)}(\xi_k)=\int_{-\infty}^{\infty}w(t)r(t+\xi_k)dt \tag{10a}$$

Using (2a) and (2b), considering the k^{th} frame, and assuming the reference monocycles are timed at $T^{(s)}(t^{(s)}_{k})=kT_f$:

$$\begin{aligned}g^{(s)}(\xi_k) &= \int_{-T_D+t^{(s)}_{k}}^{T_D+t^{(s)}_{k}}A_wA_rw(t-\bar{T}^{(m)}(kT_f)-\tau_{m,s}-\rho_{m,s})r(t-\bar{T}^{(s)}(kT_f))dt+n^{(s)}_{k} \\ &=\breve{g}_o\cdot\xi_k\ +\ n^{(s)}_{k}\end{aligned} \tag{10b}$$

where $2T_D$ is the integration time of the detector, and

$$\breve{g}_o=(dg(\xi)/d\xi)|_{\xi=0} \tag{10c}$$

$$\xi_k=\tau_{m,s}+\rho_{m,s}+a^{\delta}_{1}kT_f+d^{\delta}-\mu_{(k)} \tag{10d}$$

$$n^{(s)}_{k}=A_r\int_{-T_D+t^{(s)}_{k}}^{T_D+t^{(s)}_{k}}n(t)r(t-\bar{T}^{(s)}(kT_f))dt\,. \tag{10e}$$

The second line of (10b) is obtained assuming the timing detector operates at the linear region of its detector characteristic, i.e, the timing error ξ fluctuates about the stable equilibrium point at $\xi=0$ such that $g(\xi)$ around $\xi=0$ is approximated by $g(\xi)=\xi\cdot\breve{g}_0$. The output of the timing detector becomes:

$$x_k=\tau_{m,s}+\rho_{m,s}+a^{\delta}_{1}kT_f+d^{\delta}+n^{(s)}_{k}/\breve{g}_o-\mu_{(k)} \tag{11}$$

where without lost of generality, K_D (the detector gain as shown in Fig. 2), is commonly chosen to make the effective gain of the timing detector equal to 1, i.e., $K_D=1/\breve{g}_o$. Further, it is assumed that the transceivers in the network are stationary during time transfer and the

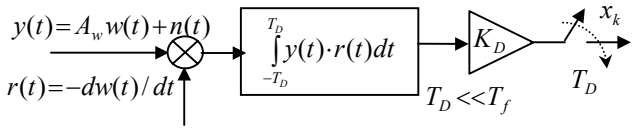

Figure 2: Illustration of correlator timing error detector. The input signal and the reference signal is multiplied and integrated over a period of $2T_D$ to obtain the timing error output.

amplitude of the reference signal A_r is also set to one. Equation (11) has the same generic form as the ToA of (8a) and (8b).

Without computing any matrix inverse, the LS estimators of γ and ζ can then be shown to be [16]:

$$\hat{\gamma}_{LS} = (12\sum_{k=0}^{K-1} k \cdot x_k)/(K(K^2-1)) - 6\sum_{k=0}^{K-1} x_k/(K(K+1)) \quad (12a)$$

$$\hat{\zeta}_{LS} = (2(2K-1)\sum_{k=0}^{K-1} x_k)/(K(K+1)) - (6\sum_{k=0}^{K-1} k \cdot x_k)/(K(K+1)) \quad (12b)$$

if K frames are used, $x_k = \gamma k + \zeta + \mathsf{v}_k$ (x_k is given by (11)), where $\gamma = a_1^{\delta} T_f$, $\zeta = d^{\delta} + \tau_{m,s} + \rho_{m,s}$ and v_k is the measurement noise with zero mean. From (12a) and (12b) the estimators are unbiased, i.e., $\{\mathrm{E}\{\gamma - \hat{\gamma}_{LS}\} = 0$, $\mathrm{E}\{\zeta - \hat{\zeta}_{LS}\} = 0\}$ and the estimation variance σ_{γ}^2 and σ_{ζ}^2 are bounded as follows:

$$\sigma_{\hat{\gamma}_{LS}}^2 = \mathrm{E}\{|\gamma - \hat{\gamma}_{LS}|^2\} \geq 12\sigma_{\mathsf{v}}^2 / (K(K^2-1)) \quad (13a)$$

$$\sigma_{\hat{\zeta}_{LS}}^2 = \mathrm{E}\{|\zeta - \hat{\zeta}_{LS}|^2\} \geq (2(2K-1)\sigma_{\mathsf{v}}^2) / (K(K+1)) \quad (13b)$$

where σ_{v}^2 is the variance of the measurement noise.

According to [16], since mapping from the parameters to be estimated (γ, ζ) to the measurement space is deterministic and v are independently identical distributed (i.i.d.) with zero mean, then the LS estimator is unbiased and an efficient estimator within the class of linear estimators. Indeed, [17] has independently shown that (13a) is the Cramer-Rao bound for estimating the frame frequency difference.

ADDITIVE NOISE AND OSCILLATOR JITTER

The measurement noise, $\varepsilon_{(k)}^{\{a,b,c\}}$ can be attributed to additive noise in the channel and error due to multipath self-interference. As pointed out earlier, the bias on the ToA measurements attributed to multipath self-interference is assumed negligible for UWB impulses of sufficiently narrow width [8], and hence it is ignored here. Therefore in the LS estimators, from (10), (11) and (8):

$$\mathsf{v}_k = \varepsilon_{m,s(k)} / \breve{g}_o - \mu_{(k)} = n_{m,s(k)} / \breve{g}_o - \mu_{(k)} \quad (14)$$

whereby no distinction is make between the master and slave timing detector characteristics. In this section, $n_{(k)}$ of (14) and random phase noise $\varphi(t)$ of the oscillators are analyzed while $\rho_{m,s}$ is analyzed in the next section.

If the master and slave transmit with equal energy and there is reciprocity of the propagation channel, $n_{(k)} / \breve{g}_o$ are i.i.d. with variance denoted as $\sigma_{m,s(n)}^2$. This timing jitter can be bounded using the Cramer Rao bound given in [1] if $r(t) = -dw(t)/dt$:

$$\sigma_{m,s(n)}^2 \geq 1 / (\Theta_{m,s} \overline{\omega^2}) \quad (15)$$

where $\Theta_{m,s} = A_w^2 / (N_o/2)$ is the SNR at receiver, A_w^2 is the received signal energy, $W(f)$ is the Fourier transform of $w(t)$ defined in (2) and $\overline{\omega^2} = \int_{-\infty}^{\infty} \omega^2 |W(\omega)|^2 d\omega / 2\pi$ is the effective squared bandwidth. This bound is optimistic because matched filter UWB receivers are hard to build.

Next, assuming the phase noise of oscillators in the network are i.i.d. with Power Spectral Density (PSD) $S_{\varphi}(\omega)$, the first structure function of the phase noise process is given in [2] and [15]:

$$\begin{aligned} D_{\varphi^{(s)}}^1(t) &= \mathrm{E}\left\{\left|\varphi^{(s)}(t) - \varphi^{(s)}(0)\right|^2\right\} \\ &= \frac{2}{\pi}\int_{-\infty}^{\infty} \sin^2(\omega t/2) S_{\varphi^{(s)}}(\omega)\, d\omega \leq \frac{2}{\pi}\int_{-\infty}^{\infty} S_{\varphi^{(s)}}(\omega)\, d\omega \end{aligned} \quad (16)$$

Let $\sigma_{\phi^{(s)}}^2 = 2\int_{-\infty}^{\infty} S_{\varphi^{(s)}}(\omega)\, d\omega / (\pi\omega_o^2)$ and to be conservative the upper bound of (16) will be used to determine the bound on the jitter in the system instead of the time interval dependent structural function. Thus the variance of v_k is:

$$\sigma_{m,s(\mathsf{v})}^2 \geq \sigma_{m,s(n)}^2 + 2\sigma_{\phi}^2 . \quad (17)$$

where it is assumed that the phase noise statistics of all transceivers are i.i.d.. The factor 2 of σ_{ϕ}^2 arises as $\sigma_{\mu_{(k)}}^2 = (D_{\varphi^{(m)}}^1(t) + D_{\varphi^{(s)}}^1(t))/\omega_o^2$. More details on characterizing the oscillator phase instabilities using structure function can be found in [15]. As put forth in [15], $\varphi(t)$ is not stationary (the N$^{\text{th}}$ increment of $\varphi(t)$ is stationary) and thus does not possess a power spectral density in the usual sense. To avoid this difficulty, [15] defined $S_{\varphi}(\omega) = S_{\dot{\varphi}}(\omega)/\omega^2$ where $\dot{\varphi}(t) = d\varphi(t)/dt$ and $\dot{\varphi}(t)$ is a stationary, zero mean random process. The same definition is adopted in this paper.

EFFECT OF NLOS MEASUREMENTS

The received NLOS signals refer to signals scattered from scattering centers distributed around the transceivers or signals, which may be scattered rays themselves, that have gone through blockages in their propagation paths. It is assumed, for convenience and lacking definitive results in the literature on UWB signal propagating through materials, that retardation of the LOS signal passing through blockages is negligible compared with additional propagation time via scattering. This assertion needs further scrutiny when more propagation data becomes available in the open literature. If the propagation path of a LOS signal is blocked resulting in low SNR at the receiver and the signal not detected at the receiver, the ToA measurement is derived from scattered NLOS signals.

There exists various scatter models such as ring, uniform, circular and elliptical [10]. Of interest is the

Gaussian scatter model which assumed variations of scatter density about the transmitter are given by a Gaussian distribution with standard deviation σ_g, and signals undergo single scattering from the scatter region before arriving at the receiver. It is adopted here due to its ability to model environments with different degrees of scattering by adjusting σ_g [10]. Reference [10] has also derived the probability density function of the total path length in time, τ traveled by the signal, assuming the scatters are symmetrically distributed about the line joining the transmitter and receiver. This density is denoted herein as $P_{go}(\tau|\tau_{m,s})$ where $\tau \geq \tau_{m,s}$.

To proceed further, $\rho_{m,s}$ of (2a) is written as:

$$\rho_{m,s} = \beta(\tau - \tau_{m,s}) \tag{18}$$

where $\beta \in \{0,1\}$ is an independent random variable that takes on a value 0 with probability $1-p_\beta$ for a LOS signal, which removes the singularity in $P_{go}(\tau|\tau_{m,s})$ at $\tau=\tau_{m,s}$, and a 1 with probability p_β otherwise. The probability p_β indicates the chances of the received signal being a NLOS signal. The following statistics are of interest:

$$\overline{\rho}_{m,s} = \mathrm{E}\{\rho_{m,s}|\tau_{m,s}\} = \mathrm{E}\{\beta\}(\{\mathrm{E}\{\tau|\tau_{m,s}\} - \tau_{m,s}) \tag{19}$$

$$\sigma^2_{\rho_{m,s}} = \mathrm{var}\{\rho_{m,s}|\tau_{m,s}\} = \mathrm{E}\{\beta^2\}\mathrm{E}\{(\tau-\tau_{m,s})^2|\tau_{m,s}\} - (\overline{\rho}_{m,s})^2 \tag{20}$$

The conditional mean $\overline{\rho}_{m,s}$ and variance, $\sigma^2_{m,s}$ will be used to establish the extrema of the system. In Fig. 3, using numerical integration to evaluate $P_{go}(\tau|\tau_{m,s})$, $\overline{\rho}_{m,s}/\tau_{m,s}$ is plotted against p_β for a slave node D=10 meters away from the master. It is obvious that the bias is significant even for scatter region having small σ_g. Therefore some form of signal processing, e.g., the maximum likelihood-estimation maximization algorithm of [11] can be used to mitigate the NLOS bias. Alternatively, the redundancy available in the time transfer scheme of the SIN can be exploited via the 'roving' master concept to be introduced later to possibly alleviate NLOS error by providing alternative signal propagation path for time transfer to overcome blockages.

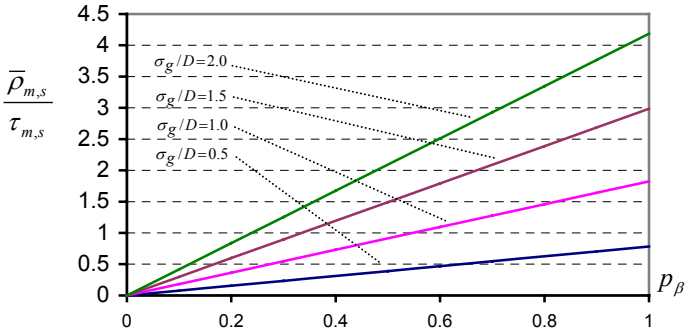

Figure 3: Normalized bias in ToA due to NLOS measurements as a function of probability of signal being blocked, p_β. The LOS distance between transmitter and receiver is D=10 meters.

PERFORMANCE

To evaluate the timing jitter of the proposed synchronization scheme, from (8), the ToAs needed for time transfer from master (m) to slave (s) are re-expressed as follows:

$$\Omega^a_{m,s(k)} = \zeta^a_{m,s} + \gamma^a_{m,s}\cdot k + \mathsf{v}^a_{m,s} \tag{21a}$$

$$\Omega^b_{s,m(z,j)} = \zeta^b_{s,m} + \gamma^b_{s,m}\cdot\theta_{up(z,j)} + \mathsf{v}^b_{s,m} \tag{21b}$$

where $\mathsf{v}^a_{m,s} = -\mu_{(k)} + n_{m,s(k)}/\breve{g}_o$ and $\mathsf{v}^b_{s,m} = \mu_{(\theta_{up(z,j)})} + n_{s,m(z,j)}/\breve{g}_o$ are the zero mean measurement noises, and $\gamma^a_{m,s} = -\gamma^b_{s,m} = a_1^\delta T_f$, $\zeta^a_{m,s} = \tau_{m,s} + d^\delta + \rho_{m,s}$, $\zeta^b_{s,m} = \tau_{s,m} - d^\delta + \rho_{s,m}$. Also,

$$\Omega^c_{m,s(z,j,i)} = \zeta^c_{m,s} + \gamma^c_{m,s}\cdot(\theta_{dn(z,i)} - \theta_{up(z,j)}) + \mathsf{v}^c_{m,s} \tag{21c}$$

where $\zeta^c_{m,s} = \tau_{m,s} + \tau_{s,m} + \rho_{m,s} + \rho_{s,m}$, $\gamma^c_{m,s} = a_1^\delta T_f$, and $\mathsf{v}^c_{m,s} = (n_{m,s(z,i)} + n_{s,m(z,j)})/\breve{g}_o - \mu_{(\theta_{dn(z,i)})} + \mu_{(\theta_{up(z,j)})}$. The quantity $(\theta_{dn(z,i)} - \theta_{up(z,j)}) = (N-1+i-j)K_r$ is independent of frame indices. Taking note that the slave transceiver only has measurements $\Omega^a_{m,s(k)}$ and $\Omega^c_{m,s(z,j,i)}$, and there are various approaches to estimate ζ and γ from these measurements. Here we proposed using the LS estimators on $\Omega^a_{m,s(k)}$ to obtain an estimate $\hat{\gamma}^a_{m,s}$ of $\gamma^a_{m,s}$. From (12), for $k \in \{0,\ldots,K_s-1\}$, the estimation variance is bounded by:

$$\sigma^2_{\hat{\gamma}^\delta_{m,s}} = \sigma^2_{\hat{\gamma}^a_{m,s}} = \mathrm{E}\{|\gamma^a_{m,s} - \hat{\gamma}^a_{m,s}|^2\} \geq 12\sigma^2_{m,s(\mathsf{v})}/(K_s(K_s^2-1)) \tag{22}$$

With $\hat{\gamma}^a_{m,s}$ computed at the slave, it is used to correct the drift rate of the slave's local oscillator immediately instead of at the end of the down-link ranging pulses. This is to support more nodes in the network. The timing equation after receiving the down-link ranging pulses, with (21a) adjusted by $\hat{\gamma}^a_{m,s}$ before substituting into (6), becomes:

$$\vartheta_{m,s(k,z,j,i)} = -d^\delta + \frac{\rho_{s,m} - \rho_{m,s}}{2} + \Xi_{(k,j,i)}(a_1^\delta T_f - \hat{\gamma}^a_{m,s}) + \mathsf{v}_{(k,z,j,i)} \tag{23}$$

where $\Xi_{(k,i,j)} = ((N-1+i-j)K_r - 2k)/2$ is a function of the frame index k, and $\mathrm{E}\{\mathsf{v}^2_{(k,z,j,i)}\} \geq (3/2)(1/\Theta_{m,s}\overline{\omega^2} + 2\sigma^2_\phi)$.

The estimate $\hat{d}^\delta_{m,l}$ of the initial offset $d^\delta_{m,l}$ between a pair of oscillators is obtained from (23) by applying LS estimation on $\vartheta_{m,s}$ or taking its statistical average, i.e,

$$\hat{d}^\delta_{m,s} = \textstyle\sum_{k=0}^{K-1}\vartheta_{m,s(k,z=k,j,i)}/K \tag{24}$$

for $K = K_s = K_r >> 1$. For $i=j$, the mean and variance of (24) is, assuming $n(t)$ and oscillator phase noises are i.i.d.:

$$\mathrm{E}\{\hat{d}^\delta_{m,s}\} = d^{(s)} - d^{(m)} + (\rho_{s,m} - \rho_{m,s})/2 \tag{25a}$$

$$\sigma^2_{\hat{d}^\delta_{m,s}} \geq 3\left((N-2)^2 + 1/2\right)(1/\Theta_{m,s}\overline{\omega^2} + 2\sigma^2_\phi)/K \tag{25b}$$

The performance of the SIN is examined next considering estimation variances on d^δ and oscillator

drift, a_1^{δ}. Numerical values for the phase noise depends on the choice of the oscillator and $S_{\varphi}(\omega)$ is usually specified as single side band noise in dB relative to the oscillator carrier (dBc)[13]. Instead of specifying the oscillator phase noise, the normalized standard deviation $\sigma_{\hat{d}^{\delta}}/\sigma_w$ (excluding $\sigma^2_{\rho_{m,s}}$ of (20)) where σ_w is the approximate width of $w(t)$, is plotted in Fig. 4 vs. K for various σ_{ϕ}^2. Also, assuming $K=K_s$ and perfect power control in the network such that $\Theta_{m,s}$ is kept at 30 dB. Note that $\sigma_{\phi}=10^{-12}$ is 0.001 of a nsecs. The received UWB monocycle $w(t)$ is modeled using the n^{th} order Gaussian derivative waveform [7],[8]. We choose a $w(t)$ with a spectrum that fits into the FCC indoor mask with pulse width (main lobe) of about 0.067 nsecs. The NLOS jitter $\sigma^2_{\rho_{m,s}}$ at $\sigma_g/D=2$ and $p_{\beta}=1$ is $6.7\text{x}10^{-15}$ sec^2 ($\sigma_{\rho_{m,s}}/\sigma_w \approx 1221$) at D=10 m is significantly larger than the values plotted in Fig. 4 for additive noise. In Fig. 4, $\sigma_{\hat{\gamma}^{\delta}_{m,s}}/\sigma_w$ is also plotted. There is hardly any lowering of timing jitter for σ_{ϕ} better than 10^{-13}. It illustrates that for a specific $\Theta_{m,s}$, as σ_{ϕ} decreases until $\sigma^2_{m,s(n)} >> 2\sigma^2_{\phi}$, then $\sigma^2_{m,s(\text{v})}$ is dominated by $\sigma^2_{m,s(n)}$ and oscillator with even smaller phase noise would not reduce the timing jitter significantly. Note that $\sigma^2_{\gamma^{\delta}}$ decreases as K^3 while $\sigma^2_{d^{\delta}}$ decreases with K.

In the absence of noise and interference, the differences in the oscillator drift a_1^{δ} and initial offset d^{δ} between master and slaves determine the number of nodes N we can place in the network such that UWB impulses would arrive at the designated time slots and the TDMA scheme is not violated. Further, to avoid inter-frame interference, let $\tau' = \tau + \tau_{rms}$ where τ_{rms} is the root-mean-square(rms) delay spread of the channel while ignoring NLOS error. The first bound on N can be deduced from the requirement that ToA_1 needs to be within the designated receiving time slot of the slave transceiver, i.e., $0<\Omega^{a}_{m,s(K_s-1)}<a_1^{(s)}T_f$. Assuming $K_s=K_r=K$ leads to:

$$a_1^{\delta}(K-1)T_f+\tau'>d^{(s)}-d^{(m)} \quad (26a)$$

$$d^{(s)}-d^{(m)}>a_1^{\delta}(K-1)T_f+\tau'-a_1^{(s)}T_f \quad (26b)$$

Placing similar restriction on ToA_2 for $a_1^{\delta}KT_f>0$ and considering $j=N$, $z=K-1$ in (8b), leads to:

$$N>(-d^{\delta}+a_1^{\delta}T_f+\tau'-a_1^{(m)}T_f)/(a_1^{\delta}KT_f) \quad (27a)$$

$$N<(a_1^{\delta}T_f-d^{\delta}+\tau')/(a_1^{\delta}KT_f) \quad (27b)$$

For $a_1^{\delta}KT_f>0$, $z=K-1$, the bound on ToA_3 is $0<\Omega^{c}_{m,s(z,i,j)}<a_1^{(s)}T_f$, which leads to the inequalities:

$$N>2\tau'/(-a_1^{\delta}KT_f)-i+j+1 \quad (28a)$$

$$N<(a_1^{(s)}T_f-2\tau')\big/(a_1^{\delta}KT_f)-i+j+1 \quad (28b)$$

The corresponding inequalities on N if $a_1^{\delta}KT_f<0$ are derived similarly. The upper bound on N for master-slave time transfer is obtained by combining the inequalities (26), (27) and (28) and their dual when $a_1^{\delta}KT_f<0$.

To obtain numerical values on N, the communicating range of the UWB transceiver is assumed to be between 1 and 10 m, and thus τ is in the order of $3\text{x}10^{-8}$ secs. The IEEE 802.15.3a multipath channel model for UWB signals specified an rms delay spreads on the order of 10 nsec. In Fig. 5, we plotted the upperbound on N with $\tau' \in \{10^{-8}, 2\text{x}10^{-8}, 3\text{x}10^{-8}\}$ secs assuming $T_f \in \{10^{-3}, 10^{-4}\}$ secs and $N>0$, $d^{(m)}=d^{(s)}$, $a_1^{(m)}=1$ and $a_1^{(s)}=a_1^{(m)}\pm\eta$ where η is a small number that represents the largest difference in drift between pair of oscillators in the network. We have arbitrarily let K=512 and $i=j$ in Fig. 5. It illustrates that at $\eta=10^{-9}$, $\tau'=3\times10^{-8}$ and $T_f=10^{-3}$, $N<60$. In [12], it is reported that precision Quartz oscillator has a normalized drift $\Delta\omega/\omega_o$ of 10^{-10} per day.

It is essential that nodes in the network are in some form of coarse synchronization to ensure $d^{(m)} \approx d^{(s)}$ before the start of the SIN synchronization process described above. The synchronization pulses from the master to slave at the first time slot can be used to bring $a^{(m)} \approx a^{(s)}$ to the required tolerance for a specific N using the approaches mentioned earlier and with sufficiently large K_s.

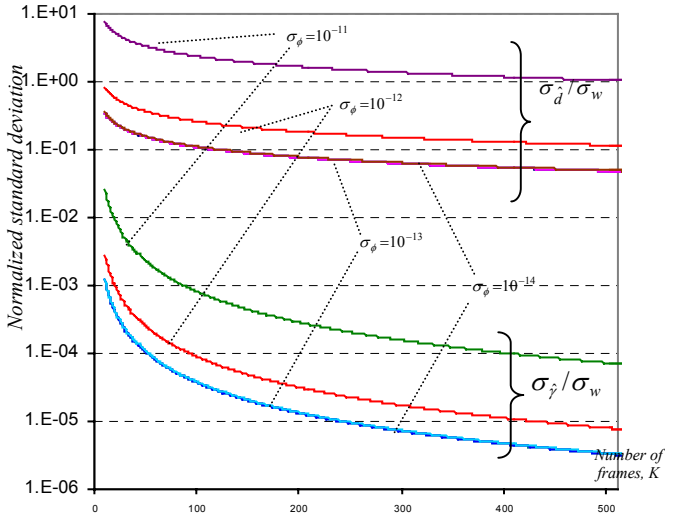

Figure 4: Using (22) and (25), lower bound on accumulated timing jitter due to additive noise and oscillators' phase noise as a function of K for various values of σ_{ϕ} at $\Theta_{m,s}=30dB$, $\zeta=0$ and $\gamma=0$. Note that NLOS jitter is not included. Plots of $\sigma_{\phi}=10^{-13}$ and $\sigma_{\phi}=10^{-14}$ are very close to each other and are not distinguishable in the figure. Number of nodes in network, N=60.

To obtain numerical values on N, the communicating range of the UWB transceiver is assumed to be between 1 and 10 m, and thus τ is in the order of $3\text{x}10^{-8}$ secs. The IEEE 802.15.3a multipath channel model for UWB signals specified an rms delay spreads on the order of 10 nsec. In Fig. 5, we plotted the upperbound on N with $\tau' \in \{10^{-8}, 2\text{x}10^{-8}, 3\text{x}10^{-8}\}$ secs assuming $T_f \in \{10^{-3}, 10^{-4}\}$ secs and $N>0$, $d^{(m)}=d^{(s)}$, $a_1^{(m)}=1$ and $a_1^{(s)}=a_1^{(m)}\pm\eta$ where η is a small number that represents the largest difference in drift between pair of oscillators in the network. We have arbitrarily let K=512 and $i=j$ in Fig. 5. It illustrates that at $\eta=10^{-9}$, $\tau'=3\times10^{-8}$ and $T_f=10^{-3}$, $N<60$. In [12], it is reported that precision Quartz oscillator has a normalized drift $\Delta\omega/\omega_o$ of 10^{-10} per day.

It is essential that nodes in the network are in some form of coarse synchronization to ensure $d^{(m)} \approx d^{(s)}$ before the start of the SIN synchronization process described above. The synchronization pulses from the master to slave at the first time slot can be used to bring $a^{(m)} \approx a^{(s)}$ to the required tolerance for a specific N using the approaches mentioned earlier and with sufficiently large K_s.

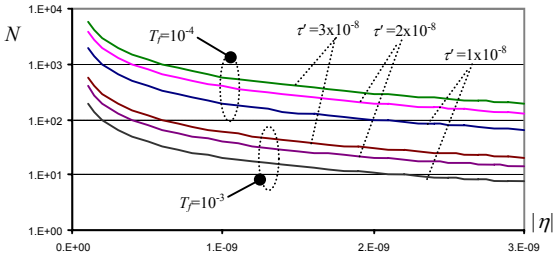

Figure 5: The upper bound on the number of nodes in the network N as a function of difference in oscillator drift η. The y-axis is in log scale assuming there is no jitter or measurement errors and K=512.

'ROVING' MASTER SYNCHRONOUS NETWORK

The synchronization scheme described in previous Sections is a master-slave synchronization approach with TDMA among transceivers in the network. The concept of a 'roving' master, which builds upon the master-slave time transfer, is to let each transceiver in the network takes a turn as the master node (Fig. 6). In applications where the transmission range of each node is limited by power constraint, the 'roving' master concept works much like a terrestrial cellular system with numerous base stations each covering a small local area. Each node in the SIN is capable of being the master (base station) to exchange timing with other nodes (slaves ≡ mobile terminals) that are in close proximity with it. It first synchronized itself with the timing of a designated lead-master node, i.e., the node that is tasked to start the synchronization process as the first master node. Then when it becomes the master, it propagates this timing to other nodes that the lead-master on its own could not reach. Thus extending the geographical coverage of the synchronous network and overcoming blockages in signal paths (Fig. 6).

If there are N nodes in a network, a single synchronization session of master-slave will take $(2(N-1)K_r+K_s)$ time frames. A complete roving of all N transceivers in the network will take $(2N-1)NK$ time frames if $K_s=K_r=K$. More importantly, at the end of one roving cycle, each transceiver in the network would have taken $(N-1)$ measurements of $(\Omega^a,\Omega^b,\Omega^c)_{m,s}$. If the ToA measurements are weighted (with weight $\alpha_{m,s}$, $\sum_{m=1,m\neq s}^{N}\alpha_{m,s}=1, \forall s$ and (m) the roving master) [3] according to some criteria such as received signal strength, the timing adjustments at each node can be obtained as a weighted combination of inputs from all other nodes in the network. Thus we have a mutual synchronous network, which is characterized by every oscillator in the network contributing to the settled timing of the network, i.e., every node has a say and contributes to the timing whenever it is acting as the master node. The relative merits of master-slave and mutual synchronous network with narrowband transceivers for communication are discussed in [3][5]. A detail analysis of the 'roving' master and the mutual synchronous SIN is in progress.

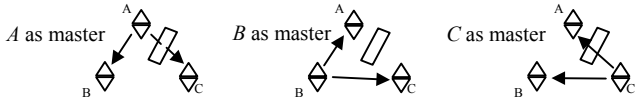

Figure 6: 'Roving' the master to overcome blockages in signal paths. The 'arrows' depicts the master sending out synchronizing pulses to the slaves.

In conclusion, this paper proposed a synchronization scheme for an impulse network (SIN). The analysis aims to predict the performance of the SIN taking into consideration additive channel noise, oscillator phase noise and NLOS measurement error. Preliminary simulation results (omitted herein due to space constraint) agree well with the theoretical analysis described hereabove.

REFERENCES

[1] H. Meyr, M. Moeneclaey and S. A. Fechtel, *Digital Communication Receivers – Synchronization, Channel Estimation, and Signal Processing*, Wiley, 1998.

[2] Heinrich Meyr and Gerd Ascheid, *Synchronization in Digital Communications–Volume 1, Phase-, Frequency-Locked Loops, and Amplitude Control*, Wiley 1990.

[3] W. C. Lindsey, F. Ghazvinian, W. C. Hagmann and K. Dessouky, "Network Synchronization", *Proc. IEEE*, October 1985.

[4] Donald B. Sullivan and Judah Levine, "Time Generation and Distribution", *Proc. IEEE*, vol. 79, No. 7, July 1991.

[5] S. B. Cefriel, "A Historical Perspective on Telecommunications Network Synchronization", *IEEE Commun. Mag.*, June 1998.

[6] Franco Mazzenga, Francesco Vatalaro and C. E. Wheatley III, "Performance Evaluation of a Network Synchronization Technique for CDMA Cellular Communications", *IEEE Trans. Wireless Commun.*, vol. 1, No. 2, April 2002.

[7] Chee-Cheon Chui and Robert A. Scholtz, "Optimizing Tracking Loops for UWB Monocycles", *Proc. IEEE Globecom*-2003.

[8] Chee-Cheon Chui and Robert A. Scholtz, "Tracking UWB Monocycles in IEEE 802.15 Multi-path channels", *Proc. Asilomar Conf. Signals, Systems, and Computers,* 2003.

[9] Joon-Yong Lee and R. A. Scholtz, "Ranging in a Dense Multipath Environment using an UWB Radio Link", *IEEE J. Select. Areas Commun.*, vol. 20, No. 9, Dec 2002.

[10] R. Janaswamy, "Angle and Time of Arrival Statistics for the Gaussian Scatter Density Model", *IEEE Trans. Wireless Commun.*, vol. 1, No. 3, July 2002.

[11] S. Al-Jazzar & J. Caffery, Jr, "ML & Bayesian TOA Location Estimators for NLOS Environments", *Proc. IEEE VTC,* 2002-Fall.

[12] J. R. Norton and J. M. Cloeren, "Brief History of the Development of Ultra-Precise Oscillators for Ground and Space Applications", *IEEE International Frequency Control Symposium*, 1996.

[13] W.F.Walls and F.L.Walls, "Computation of Time-Domain Frequency Stability and Jitter from PM Noise Measurements", *IEEE Frequency Control Symposium and PDA Exhibition*, 2001.

[14] Yao-Win Hong and Anna Scaglione, "Time Synchronization and Reach-Back Communications with Pulse-coupled Oscillators for UWB Wireless Ad-hoc Network", *IEEE International Conference on Ultra Wideband Systems and Technologies*, 2003.

[15] W. C. Lindsey and C. M. Chie, "Theory of Oscillator Instability Based Upon Structure Functions", *Proc. IEEE*, Dec 1976.

[16] J. M. Mendel, *Lessons in Estimation Theory for Signal Processing, Communications, and Control*, Prentice Hall, 1995.

[17] Antonio A. D'Amico and Umberto Mengali, "Frame Frequency Estimation in Ultra-Wideband Systems", 2004, unpublished.